PERGAMON

Vision Research 42 (2002) 211–226

Vision Research

www.elsevier.com/locate/visres

Cues and strategies for color constancy: perceptual scission, image junctions and transformational color matching

Byung-Geun Khang *, Qasim Zaidi

SUNY College of Optometry, 33 W 42nd Street, New York, NY 10036, USA

Received 13 January 2001; received in revised form 8 June 2001

Abstract

The identification of objects, illuminants, and transparencies are probably the most important perceptual functions of color. This paper examines the effects of perceptual scission, image junctions, color adaptation, and color correlations on identification. Simulations of natural illuminants, materials, and filters were used in a forced-choice procedure to simultaneously measure thresholds for identifying filters and objects across illuminants, and discrimination thresholds within illuminants. In the vast majority of the cases, if observers could discriminate within illuminants they could identify across illuminants. Since results were similar for identical color distributions, whether transparency cues like X-junctions were present or not, the primary cues for color identification were systematic color shifts across illuminants. These color shifts can be well described by three-parameter affine transformations, and the parameters can be derived from differences and ratios of mean chromaticities. A strategy based on post-transformation color matching predicts generally accurate identification despite perceptible color shifts, and also provides plausible reasons for those few conditions where identification thresholds are significantly higher than discrimination thresholds.

Keywords: Color constancy; Transparency; Scission; Transformational color matching; Color discrimination

1. Introduction

Possibly the most important perceptual functions of color are the identification of objects across illuminants and through transparencies, of transparencies across objects and illuminants, and of illuminants across objects. Consider a display like Fig. 1(a). The colors of the ellipses are calculated from the reflectances of a set of natural and man-made materials (Vrhel, Gershon, & Iwan, 1994), seen under two different natural illuminants, zenith skylight and direct sunlight (Taylor & Kerr, 1941). This is an extreme example of the situation that occurs when a large object like a mountain blocks sunlight from parts of a scene which then reflect the sky. The question arises whether an observer can separate each pixel of the image into a color component intrinsic to the material surface and an extrinsic color component contributed by the illuminant (Arend, 1994; Mausfeld, 1998). If this were possible, an observer could identify materials of similar reflectance across illuminants despite perceivable color differences, leading to constancy of what Lichtenberg called the inferred colors of objects (Lichtenberg, 1793).

Since color signals from individual pixels do not contain separable information about the characteristics of the material and the illuminant, color identification requires the use of geometrical and color relationships across the visual image. In Fig. 1(a), the presence of an illumination change is signaled both by geometric and color cues. The perceptible geometric cue is the vertical division in the center of the image across which boundaries of ellipses continue undisturbed. In terms of image properties, the main cues are the X-junctions lined along the boundary between the two illuminants. The perceptible color cues are the relatively more orange or blue–green colors of the ellipses in the two vertical halves. In terms of physiological color mechanisms, the main cues are that each of L, M, and S cone absorptions from the materials under one illuminant are almost perfectly correlated with absorptions from the materials under the other illuminant (Dannemiller,

* Corresponding author.
E-mail addresses: bgkhang@sunyopt.edu (B.-G. Khang), qz@sunyopt.edu (Q. Zaidi).

0042-6989/02/$ - see front matter
PII: S0042-6989(01)00252-8

Fig. 1. Stimulus configurations used in the experiments. Top: Two red standard filters under direct sunlight (left) and one red standard filter under zenith skylight (top right), and green test filter (bottom right). Bottom: Filtered regions were rotated 180°, which destroyed figural unity and color relations between filtered and unfiltered parts of materials on the boundary (same filters as above).

1993; Foster & Nascimento, 1994; Zaidi, Spehar, & DeBonet, 1997), and at the level of opponent-color mechanisms the illuminant caused shifts of material chromaticities (Mac- Leod & Boynton, 1979) can be adequately described by two-parameter affine transforms: an additive factor for the $L/(L+M)$ axis and a multiplicative factor for the $S/(L+M)$ axis (Zaidi, 2001; Zaidi et al., 1997).

In principle, an observer could use the geometric cues to locate an illuminant change and the correlated color shifts to identify materials and illuminants. Simple post-transformation color matching algorithms, using only chromatic information, have been shown to match materials with identical reflectances across illuminants and also to extract the relative chromaticities of the illuminants (Zaidi, 1998). We use "post-transformation color matching" in Ullman's (1996) sense of "transformational matching" to describe the equivalence of two sets of colors after one set has been corrected by the affine transformation.

In the case of circumscribed transparent overlays, the perceptual correlate of color separation has been called scission (Gerbino, Stultiens, Troost, & de Weert, 1990; Heider, 1933; Metelli, 1974). A surface partially overlaid by a transparent filter, spotlight, cast shadow, or fog can elicit two distinct percepts, the underlying surface and the overlaying medium, i.e. one can see not only the surface through the overlay but also the overlay itself. In Fig. 1(a), four such circular filters are simulated (KodakCC50, 1962). For most observers, there is an

immediate percept of four transparent layers over the ellipses. The perception of transparency in static 2-D displays depends on figural and color cues (Beck, 1978; Chen & D'Zmura, 1998; D'Zmura, Colantoni, Knoblauch, & Laget, 1997; Faul, 1996; Kersten, 1991; Metelli, 1974). In terms of figural cues, when two or more surfaces are partially superimposed by a transparent overlay, as the edge of the overlay crosses the border of the two surfaces, a point of intersection or an X-junction between four colored regions is created. In terms of color cues, the changes in colors at each X-junction must be constrained so as to lead the visual system to infer that the surface seen under the transparent overlay corresponds to the same surface seen directly. Such changes include those by additive, subtractive, or multiplicative color mixtures of transparent layers and background.

The scission in Fig. 1(a) is perceptually salient enough to identify the filter on the top left as 'reddish' and on the bottom right as 'greenish'. This paper examines the extent to which observers can separate and extract the spectral effects of transparent filters and identify them across illuminants and materials. In Experiment 1, we measure observers' thresholds for discriminating and identifying spectral filtering characteristics of simulated transparent overlays. It is a truism that a visual scene can be parsed in infinitely many ways. Images that evoke color transparencies provide an opportunity to test the relationship between scission into geometrically distinct layers, and scission into layers of attributed colors. In Experiment 2, we test whether discrimination and identification thresholds for spectral filtering characteristics are influenced by image geometry cues that promote perceptual transparency.

2. Experiment 1: filter identification

Identical filters will cause systematically different spectral changes under two spectrally different illuminants. When shown the effects of filtered and unfiltered illuminants on the same set of diverse materials, can an observer identify two filters with identical spectral transmittance? Using a 4AFC procedure, we measured spectral thresholds for choosing identical filters across spectrally different illuminants. As a gauge of the best achievable identification performance for each observer and each condition, the procedure simultaneously provided spectral thresholds for discriminating between filters under the same illuminant.

2.1. Methods

2.1.1. Stimuli

The stimuli were similar in appearance to those in Fig. 1(a) (angular subtense $36° \times 27°$), and simulated spectrally distinct illuminants, spectrally selective filters, and materials with a wide variety of spectral reflectances. The spectra of two daylights, direct sunlight and zenith skylight as measured by Taylor and Kerr (1941), were used to simulate illuminants for the two halves of the screen (Fig. 2(a)). The published spectra were equated for integrated energy, and though this does not reflect the generally greater radiance of sunlight, we have used them as such for the purpose of enabling the monitor to render the maximum number of materials. The transmittance spectra of six Kodak CC50 color filters (red, green, blue, yellow, magenta, and cyan) (KodakCC50, 1962), were used to simulate the double-pass transmittance of transparent overlays (due to light passing twice through an overlay, the simulated transmittance spectra are the wavelength-by-wavelength square roots of the Kodak CC50 spectra). Fig. 2 shows the spectra of the unfiltered illuminants and the illuminants double passed through the six filters. Glass filters have been measured to reflect back less than 5% of the illuminant multiplied by one plus the double-pass transmittance (Nakauchi, Silfsten, Parkkinen, & Usui, 1999). We simulated filters with zero reflectance as circular overlays of 8.8°

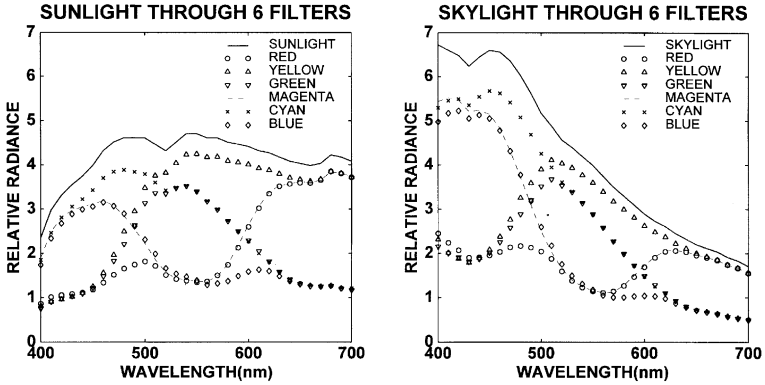

Fig. 2. Relative radiances of unfiltered and filtered sunlight and skylight (Taylor & Kerr, 1941). (a) Top solid line indicates direct sunlight, while the other six symbols represent sunlight filtered through Kodak CC50 filters (KodakCC50, 1962). (b) Top solid line indicates zenith skylight, while the other six symbols represent skylight filtered through the six filters.

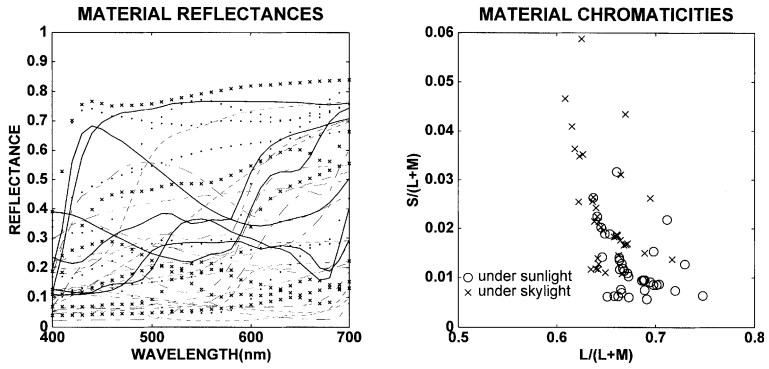

Fig. 3. (a) The reflectances of 36 materials chosen from the collection of natural and man-made objects measured by Vrhel et al. (1994): (b) MacLeod and Boynton chromaticities of the 36 objects under the two natural lights (circles for objects under sunlight and crosses for objects under skylight).

diameter. Thirty-six materials were chosen from a collection of 170 natural and man-made objects (Vrhel et al., 1994) to span the gamut of colors and were simulated as randomly sized, oriented, and overlapping ellipses (minor axis 1.8°, major axis 2.2–6.6°). A material with reflectance $R_i(\lambda)$ (Fig. 3(a)) seen under an illuminant with spectrum $E_j(\lambda)$ was rendered by calculating cone absorptions L_{ij}, M_{ij}, and S_{ij}, for the long, middle, and short wavelength sensitive cones (Smith & Pokorny, 1975):

$$\begin{aligned} L_{ij} &= \sum L(\lambda) * R_i(\lambda) * E_j(\lambda) \\ M_{ij} &= \sum M(\lambda) * R_i(\lambda) * E_j(\lambda) \\ S_{ij} &= \sum S(\lambda) * R_i(\lambda) * E_j(\lambda) \end{aligned} \tag{1}$$

where $\lambda = 400$–700 nm and "$*$" represents wavelength-by-wavelength multiplication. Distributions of MacLeod and Boynton (1979) $(L/(L+M),\ S/(L+M))$ chromaticity coordinates of the 36 materials under sunlight (circles) and skylight (crosses) are shown in Fig. 3(b). Notice that the pattern formed by the crosses is similar to the pattern formed by the circles, and in fact the patterns can be made to almost superimpose if the circles are stretched vertically and translated to the left by the appropriate constants (Zaidi, 1998). This would be an example of post-transformation color matching.

The cone absorptions for objects overlaid with a filter with double-pass transmittance $F_k(\lambda)$ were calculated by

$$\begin{aligned} L_{ijk} &= \sum L(\lambda) * R_i(\lambda) * E_j(\lambda) * F_k(\lambda) \\ M_{ijk} &= \sum M(\lambda) * R_i(\lambda) * E_j(\lambda) * F_k(\lambda) \\ S_{ijk} &= \sum S(\lambda) * R_i(\lambda) * E_j(\lambda) * F_k(\lambda) \end{aligned} \tag{2}$$

For each of the 36 materials, we calculated the $L/(L+M)$ and $S/(L+M)$ chromaticities and the sum $L+M+S$ (representing brightness) under each of the two illuminants and the six filters. The means of these values are shown in three panels in Fig. 4 (left column). Lines are used to connect the mean chromaticities from skylight (diamonds) to sunlight (circles) for unfiltered materials (open symbols) and under each filter (letters inside symbols). Notice that in the chromaticity plane (top panel) the shift from circles to diamonds is similar to the shift from crosses to circles in Fig. 3(b), i.e. with respect to the circles, the diamonds are all roughly equally translated to the left along the $L/(L+M)$ axis, and shifted up along the $S/(L+M)$ axis by a factor proportional to the value of the corresponding circle. The brightness–chromaticity planes (bottom two panels) show that the mean $L+M+S$ values are higher under sunlight by a small multiplicative constant. The standard deviations of the values along each of the color axes are shown in Fig. 4 (center and right columns). The standard deviation has been claimed to be a reasonable estimate of contrast for gray-level random dot images (Moulden, Kingdom, & Gatley, 1990) but there is no entirely satisfactory metric for perceived contrast in variegated images (Bex & Makous, 2001; Robilotto, Khang, & Zaidi, submitted). Notice that though the filters can only decrease brightness variations, they can increase or decrease chromatic variance, which is perceivable as increases and decreases in contrast. As Fig. 3(b) shows, the distributions of chromaticities in our sample were skewed. However, the skewness and kurtosis did not change appreciably across illuminants and filters.

2.1.2. Procedure

On each trial, four circular color filters were simulated to overlay four regions on the screen, two filters under one light on the left and two under the other light on the right (Fig. 1(a)). One of the six Kodak filters was chosen as the standard, $F_s(\lambda)$. Three of the filters were set identical in transmittance to the standard. The transmittance of the fourth, the test filter, $F_t(\lambda)$, was varied as a linear combination of the standard and one of the other five filters, $F_o(\lambda)$:

$$F_t(\lambda) = F_s(\lambda) + \Delta(F_o(\lambda) - F_s(\lambda)) \tag{3}$$

As the value of Δ varied from 0 to 1, the transmittance spectrum of the test filter varied from that of the stan-

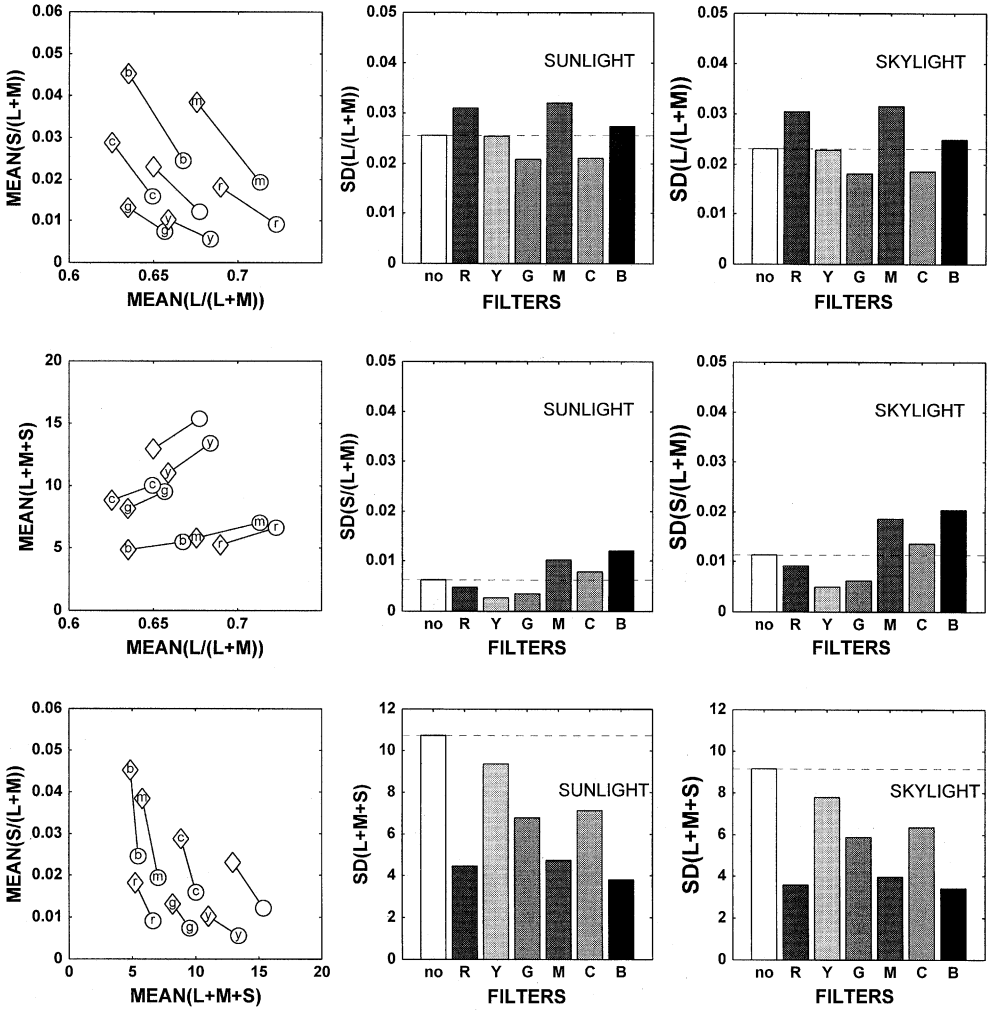

Fig. 4. Left column: Means of chromaticities of the 36 materials under the six filters under each of the two illuminants (circle for sunlight, diamond for skylight). Center & right columns: Standard deviations of the 36 objects' chromaticities under filtered or unfiltered lights.

dard filter to that of the other filter. Because of the linearity of the cone absorption calculations in Eq. (2), cone absorptions from materials under $F_t(\lambda)$ are mathematically identical to the same linear combination as Eq. (3) of the cone absorption values under $F_s(\lambda)$ and $F_o(\lambda)$. Cone absorptions under the test filters can thus be calculated directly from the values provided by Eq. (2) for the standard filters.

Observers were asked to choose which of the four filters was spectrally different by use of a switch box. They were instructed to first compare the two vertical pairs and to identify the side with the test filter as that containing distinct filters within illuminants, and then to compare the two horizontal pairs to identify the pair containing the test filter as the unlike pair across illuminants. After making the two decisions, the observer chose a switch (left or right) to indicate the first decision, and a switch direction (up or down) to indicate the location of the test. Thus, the observer's response can equivalently be conceived as a pair of independent 2AFC tasks or as identifying the test filter in a 4AFC task. No feedback was provided.

There were 60 standard–test combinations: 6 standard filters times 5 other filters times 2 daylights. Six values of delta (Δ) were run for each condition in a method of constant stimuli. Ten observations were made for each delta leading to a total of 3600 trials per observer. Measurements were spread over 30 sessions, each consisting of 120 trials: two deltas for each of the 60 conditions. Stimuli appeared on the screen with linearly increasing brightness in a 1 s ramp, were presented continuously until the observer had indicated the test filter, and then decreased in brightness linearly to complete darkness, which lasted 1 s until the next trial. The illuminant sides were assigned randomly for each trial. A single session lasted about 40 min.

2.1.3. Observers

Four observers participated in Experiment 1, all of whom had normal or corrected-to-normal visual acuity

and normal color vision. Observer BK, the first author, was aware of the nature and purpose of the experiment, but the other observers were not informed till after the conclusion of both experiments.

2.1.4. Equipment

All stimulus presentations and data collection were computer controlled. Stimuli were displayed on the $36° \times 27°$ screen (1024×768 pixels) of a Nokia Multigraph 445Xpro color monitor with refresh rate of 70 frames/s at a viewing distance of 60 cm. Images were generated by using a Cambridge Research Systems Visual Stimulus Generator (CRS VSG2/3), running in a 400-MHz Pentium II based system. Through the use of 12-bit digital–analog converters, after gamma correction, the VSG2/3 was able to generate 2861 linear levels for each gun. Any 256 combinations of the three guns could be displayed during a single frame. By cycling through precomputed lookup tables, we were able to update the entire display each frame. A Spectra-Scan PR-704 photospectroradiometer was used to measure complete spectra for the three phosphors. Phosphor chromaticities CIE(x, y) and luminances measured at the maximum luminance were (0.60, 0.34) and 11.6 cd/m^2 for the R-gun, (0.28, 0.60) and 34.2 cd/m^2 for the G-gun, (0.15, 0.07) and 4.8 cd/m^2 for the B-gun. Cone absorptions were calculated for the phosphors, and then by standard methods, cone absorptions for filtered and unfiltered materials were transformed to gun values and displayed on the screen.

2.1.5. Results

Using the methods detailed in the appendix, discrimination thresholds were estimated from the percent of side-correct responses, and identification thresholds from the percent of filter-correct responses. Identification thresholds are plotted versus discrimination thresholds for four observers in separate panels in Fig. 5. Identification and discrimination thresholds are in Δ units (Eq. (3)), and can thus be compared only within standard–other pairs. Most of the pairs of discrimination and identification thresholds fall close to or on the diagonal line, which indicates that identification thresholds were generally similar to discrimination thresholds. The points noticeably distant from the diagonal line all indicate higher identification thresholds, as should be expected. Identification thresholds have been plotted at 1.0 for those cases where thresholds were greater than the measurable range.

The appendix also presents details about two types of methods for testing the hypothesis that the probability of identification given discrimination was equal to 1.0. We used one method that essentially looks for a uniform distribution of errors for incorrect identification responses, and a second method based on comparing psychometric curves fit to side-correct and filter-correct

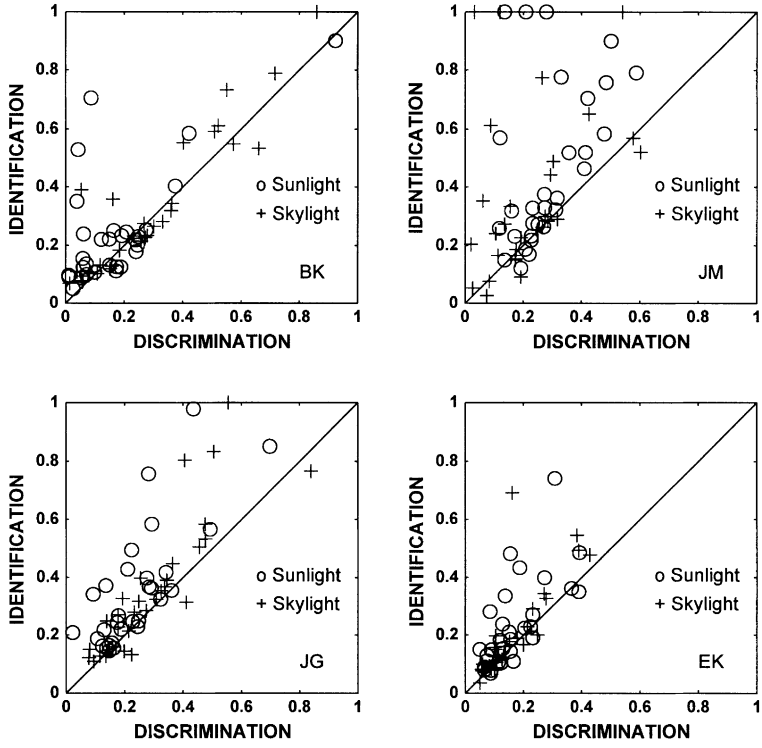

Fig. 5. Identification thresholds plotted versus discrimination thresholds separately for four observers in Experiment 1. Ordinate and abscissa are expressed in delta units of linear combination of standard and other filter transmittances.

data. For those pairs for which this hypothesis was rejected, identification threshold was taken to be significantly higher than discrimination threshold if it had the larger value. The two types of tests indicated that out of the 60 pairs of filters, identification thresholds were significantly higher than discrimination thresholds only for 8 or 3 pairs for JG, 6 or 6 pairs for BK, 4 or 10 pairs for EK, and 13 or 14 pairs for JM. In the vast majority of conditions, if an observer could discriminate between the test and standard filters under one illuminant, the observer could also identify the standard filters across the two illuminants. On the face of it, these results support a strong scission process, whereby the separation of the component intrinsic to the filter is similar enough across illuminants to enable identification.

3. Experiment 2: filter identification without X-junctions

In Experiment 1, X-junctions are formed by the continuation of ellipses across the circular edges of the filters. These X-junctions in conjunction with the systematic changes in chromaticities of ellipses partially occluded by the edge, promote a percept of transparency. In Experiment 2 we tested whether the results of Experiment 1 were influenced by the presence of cues to transparency, which could, in principle, facilitate filter scission. As shown in Fig. 1(b), by rotating the image of the circular filtered regions by 180°, we abolished both the geometric and chromatic edge-based cues to transparency, while leaving unchanged the color contents inside and outside the filters. The rotation of the overlaid regions destroyed the figural unity of objects on the boundaries between the filter and background, which is generally considered to be a requirement for perceptual transparency (Kersten, 1991). The resultant image contained a large number of T-junctions at the edges of the "filters". Some of the T-junctions were consistent with occlusion by the 'filtered region', others with occlusion by the surround.

Except for the rotation of the filtered regions, all details of Experiment 2 were identical to those of Experiment 1. Three of the four observers who participated in Experiment 1 also participated in Experiment 2. They were informed that the filtered regions were rotated 180° and asked to choose a filtered region which was different from the rest of the overlaid regions.

3.1. Results

Identification thresholds are plotted versus discrimination thresholds separately for three observers in Fig. 6. Based on the two types of tests of hypotheses, identification thresholds were significantly higher than discrimination thresholds only for 9 or 8 (BK), 11 or 9 (JM), and 9 or 9 (JG) pairs of filters. The patterns of results are similar to those in the X-junction conditions in Fig. 5. In the T-junction conditions, observers can identify filters across different illuminations almost as well as they can discriminate them under the same illumination.

In Fig. 7, thresholds in the T-junction condition are compared with thresholds in the X-junction condition. Most of the discrimination thresholds in the T-junction displays were similar to those in the X-junction displays (the top three panels of Fig. 7). No significant difference was found between 87% (JM), 78% (BK), and 75% (JG) of pairs of X- and T-junction thresholds for the three observers. This indicated that disrupting the color relations at the edge of the filter did not appreciably affect discrimination between filtered regions. Identification thresholds in the T-junction displays were also very similar to identification thresholds in the X-junction displays (the bottom three panels of Fig. 7). There was no significant difference between 99% (JM), 97% (BK), and 95% (JG) of pairs of X- and T-junction conditions for the three observers. It is therefore unlikely that identification in Experiment 1 was promoted by perceptual cues to transparency.

One way to explain the similarity of results between the two experiments is to conceive of both experiments as identification of segregated circular ensembles of materials across the two natural lights, where the spectral reflectance of each material is equal to the

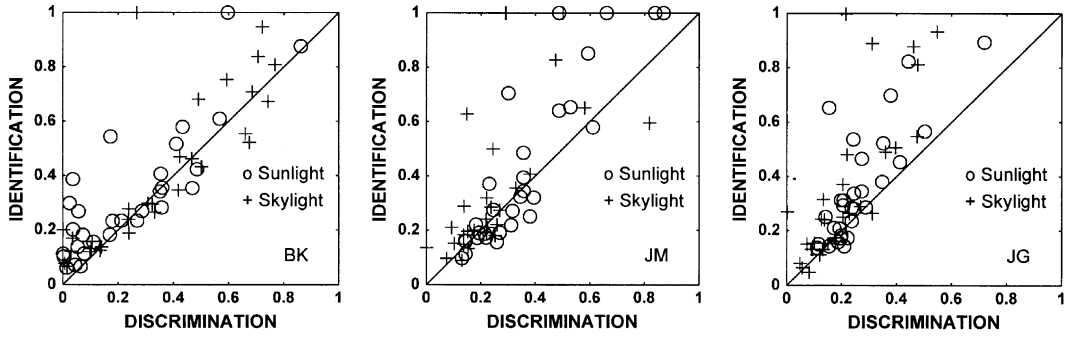

Fig. 6. Identification thresholds plotted versus discrimination thresholds separately for three observers in Experiment 2 in delta units.

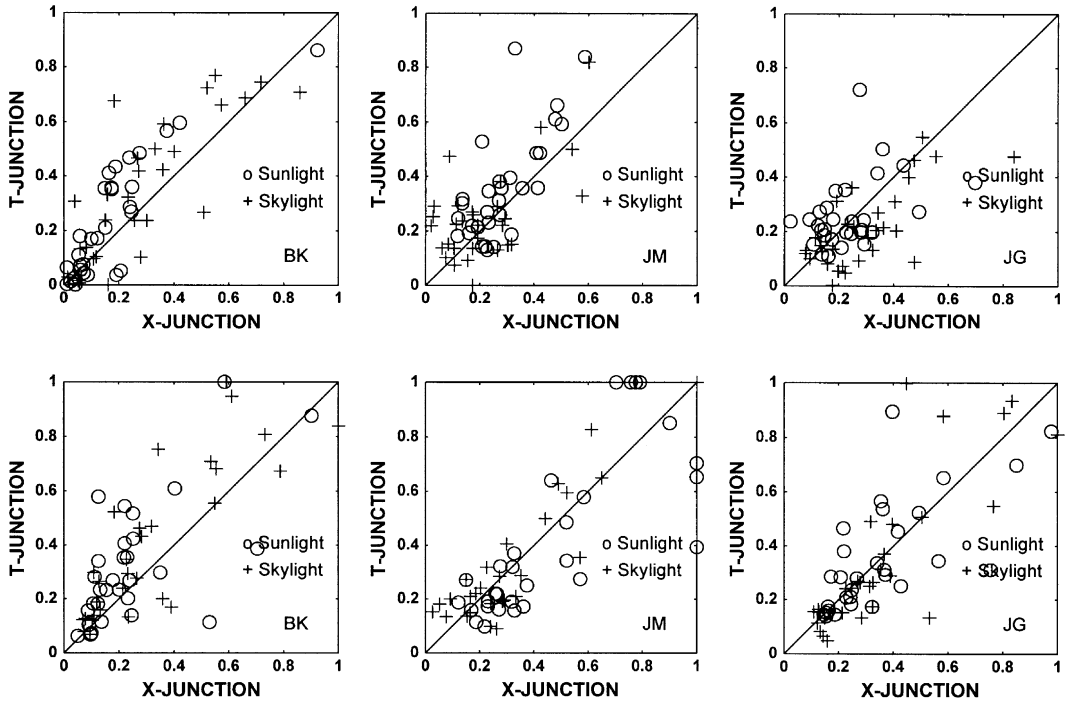

Fig. 7. Comparisons of discrimination (top) and identification (bottom) thresholds in X- and T-junction image conditions.

wavelength-by-wavelength multiplication of the spectral reflectance of the original material by the spectral transmittance of the overlaid filter. Good identification performance in the two experiments then indicates that inferred-color constancy of ensembles of materials is almost as good as color discrimination between ensembles of materials. This reconception would indicate that the X- and T-junctions serve equally well in conjunction with continuous circular borders to segment the circular ensembles from the background, and that the local color relations across the borders of the filters do not play a role in identification performance. By default, the significant clues have to be material chromaticity relations across illuminants, and these are examined in the Section 4.1.

4. Discussion

In this paper, we first tested the limits of scission as reverse optics, i.e., the separation of the perceived colors of pixels into illuminant, overlay, and material attributes. We showed that geometrical and color scission can enable an observer to identify similar overlays across different illuminants on the basis of spectral properties. Second, we showed that filter identification is not aided by geometrical cues to overlay transparency. We have introduced a performance based experimental method to measure identification and discrimination performance in complex displays. Our measure of identification is also a measure of the degree of constancy across illuminants of inferred colors of overlays or objects. The simultaneously measured discrimination thresholds provide the lowest values possible for the identification thresholds.

4.1. Cues and strategies for identification

Two aspects of the results of Experiments 1 and 2 were quite surprising to us. First, for the vast majority of conditions, identification thresholds were within probabilistic error of discrimination thresholds. In other words, whenever an observer could distinguish between two filters under one illuminant, the observer could identify which of the two filters was more dissimilar to the standard filters under the other illuminant. Second, disrupting geometric and color cues to material continuation across the edges of the filters did not make a significant change in identification thresholds. These results imply that there must be good identification cues available from the stimuli, and that these must be chromatic cues related to the distributions of colors under and outside the filters. Further, observers' neural and volitional strategies must also be close to optimal in all but the few cases where identification thresholds were significantly higher than discrimination thresholds.

Logically the first possibility to consider is that because observers were allowed as long as they liked to respond in each condition, their adaptation state settled to be equal under the two illuminant halves so that

similarly filtered regions appeared similar across illuminants. Ives (1912) used Von Kries' notion of multiplicative adaptation as a mechanism that would discount the illuminant by resetting receptor responses to be the same as under a neutral light. Nieves, Romero, Garcia, and Hita (2000) have considered adaptation at the level of opponent mechanisms. The shortcomings of such models have been detailed by Zaidi et al. (1997), and the possibility of adaptation "caused" appearance identity was contradicted by the phenomenal experience reported by all observers of our displays, i.e., the two halves of the screen always looked distinct. In a recent experiment using an asymmetric filter matching paradigm, Khang and Zaidi (submitted) have shown that identical filters do not appear identical when they overlay chromatically distinct collections of materials. This indicates that the stimuli contained chromatic cues that enabled identification across illuminants despite perceptible appearance differences.

We now examine whether a process of post-transformation color matching can account for good identification performance under the conditions of this study. Drawing an analogue between color shifts caused by illumination changes (Dannemiller, 1993; Foster & Nascimento, 1994; Zaidi et al., 1997) and those by transparent filters, Westland and Ripamonti (2000) suggested that invariant cone excitation ratios between a pair of surfaces partially covered by a filter may be the color relations necessary for the perception of transparency. In Fig. 8 we have plotted material chromaticities ($L/(L+M)$, $S/(L+M)$, $L+M+S$) under unfiltered and filtered sunlight versus corresponding chromaticities under filtered and unfiltered skylight. In addition in each of the filtered panels are plotted the mean chromaticities under the two illuminants. For the unfiltered and each of the six filtered conditions, using RG, YV, and LD as mnemonics for the $L/(L+M)$, $S/(L+M)$, and $L+M+S$ axes respectively, the transformation from sunlight to skylight can be well approximated by:

$$\begin{aligned} \mathrm{RG}_{\mathrm{sky}} &= \mathrm{RG}_{\mathrm{sun}} + \tau \\ \mathrm{YV}_{\mathrm{sky}} &= \sigma \mathrm{YV}_{\mathrm{sun}} \\ \mathrm{LD}_{\mathrm{sky}} &= \kappa \mathrm{LD}_{\mathrm{sun}} \end{aligned} \tag{4}$$

Using the index i for N objects, the RG panels show that in each panel

$$\mathrm{RG}_{i,\mathrm{sky}} = \mathrm{RG}_{i,\mathrm{sun}} + \tau + \varepsilon_i \tag{5}$$

If $\sum \varepsilon_i/N = 0$, then

$$\left(\sum \mathrm{RG}_{i,\mathrm{sky}}\right)\Big/N = \left(\sum \mathrm{RG}_{i,\mathrm{sun}}. + N\tau\right)\Big/N \tag{6}$$

therefore

$$\tau = \mathrm{mean}(\mathrm{RG}_{i,\mathrm{sky}}) - \mathrm{mean}(\mathrm{RG}_{i,\mathrm{sun}}) \tag{7}$$

Similarly, it is easily shown that, if for all i,

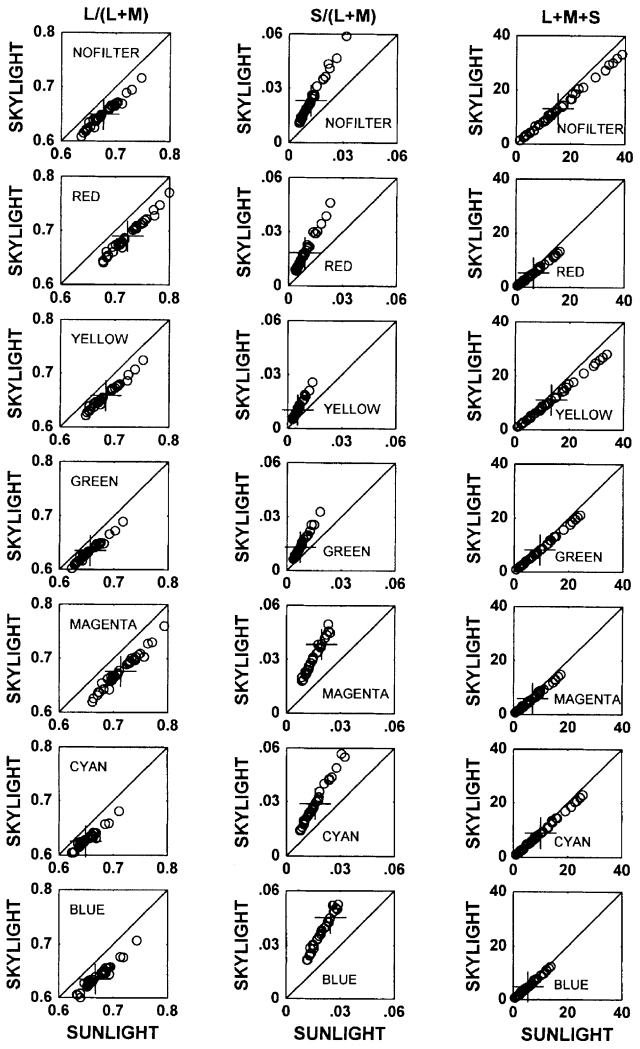

Fig. 8. Material chromaticities ($L/(L+M)$, $S/(L+M)$, $L+M+S$) under sunlight filtered by each standard filter (or no filter) versus corresponding chromaticities under skylight filtered by the same standard filter. The symbol '+' in each panel represents the mean chromaticities under the two filtered illuminants.

$$\begin{aligned} \mathrm{YV}_{i,\mathrm{sky}} &= \sigma \mathrm{YV}_{i,\mathrm{sun}} + \varepsilon_i \\ \mathrm{LD}_{i,\mathrm{sky}} &= \kappa \mathrm{LD}_{i,\mathrm{sun}} + \varepsilon_i \end{aligned} \tag{8}$$

then

$$\begin{aligned} \sigma &= \mathrm{mean}(\mathrm{YV}_{i,\mathrm{sky}})/\mathrm{mean}(\mathrm{YV}_{i,\mathrm{sun}}) \\ \kappa &= \mathrm{mean}(\mathrm{LD}_{i,\mathrm{sky}})/\mathrm{mean}(\mathrm{LD}_{i,\mathrm{sun}}) \end{aligned} \tag{9}$$

In other words, for each illuminant–filter pair, all three parameters can be estimated from appropriate differences and ratios of the coordinates of the mean material chromaticities. Table 1 shows the estimated parameters for each condition.

The similarities of the parameters across conditions point to possible strategies for filter identification in displays like Fig. 1. From the mean chromaticities of the

Table 1
Affine transformation parameters estimated from mean material chromaticities under unfiltered and filtered sunlight and skylight

	τ	σ	κ
Unfiltered	−0.0273	1.8912	0.8424
Red	−0.0333	1.9935	0.7896
Green	−0.0217	1.7760	0.8569
Blue	−0.0324	1.8421	0.8851
Yellow	−0.0249	1.8373	0.8208
Magenta	−0.0337	1.9826	0.8221
Cyan	−0.0240	1.8072	0.8830

filtered and unfiltered regions, sets of τ, σ, and κ can be estimated for the backgrounds and the two horizontal pairs of circular overlaid regions. The horizontal pair of circular regions that yields the parameters closest to those estimated from the background comparison would be chosen as the pair containing identical overlays. This class of computations would predict identification performance on a par with discrimination, because the estimated parameters from the horizontal pairs would differ significantly only if chromatic means from one of the vertical pairs differed significantly.

The similarity of estimated τ, σ, and κ within filters across illuminants is reflected by the approximate parallelism of the lines joining mean chromaticities in Fig. 4. The neural computation could thus involve searching for parallel shifts in color space without explicit estimation of τ, σ, and κ. Since, in general, the lines joining a standard filter under one illuminant to tests under the other illuminant are not parallel to the lines joining the background means (Fig. 4), identifying the dissimilar test filter should be easy. However, as the panels of Fig. 4 show, in some cases across-filter excursions are close in orientation to line joining the background means. For example, in the isoluminant chromaticity plane, a line drawn joining R means under sunlight (circle) to B means under skylight (diamond) will be almost parallel to the line joining the mean background chromaticities. In such cases one would expect identification performance to be significantly worse than discrimination.

In Table 2 we have listed the standard–test pairs of filters for which identification thresholds were significantly higher than discrimination thresholds for at least two observers in either Experiment 1 or 2. The pairs are listed according to the illuminant over the test filter, and ordered by number of observers for which the difference was significant. The main identification confusions were between the red, magenta, and blue filters. The blue and magenta filters may be confused by observers because they have substantial overlap in transmitted light, specially under skylight. However, of all pairs of filters, blue and red filters have the least overlap of their transmittance spectra. The confusions between yellow and green filters could be due to the closeness in chromaticity between the mean green under sunlight and the mean yellow under skylight.

The chromaticity means and the lines joining them reside in a three-dimensional space. The three two-dimensional depictions in Fig. 4 enable comparison of predictions on the basis of 3-D parallelisms to predictions based solely on parallelisms in the isoluminant chromaticity plane. Note that parallelism is preserved by affine transforms, so that an analysis based on parallelism in MacLeod–Boynton space will apply regardless of the color space chosen to represent the stimuli. The main complication is that MacLeod–Boynton space, like all linear transforms of metamer space, represents cone inputs and not inputs at a cortical level. Lower level adaptation processes will distort the space in a manner that is highly dependent on spatial and temporal properties of the stimuli. Since Fig. 10 shows that adaptation states are affected by the chromaticities of the overlaid regions, the distortions of color space are likely to be different for different standard–test pairs (see Section 4.4). Despite this caveat, the proposed strategy is able to predict identification confusions between blue and red filters, which have the least overlap of their transmittance spectra.

4.2. Performance based color constancy

In a letter to Goethe, Lichtenberg (1793) wrote that an object is thought to be "white", if it seems to be capable of reflecting back equally all wavelengths of the

Table 2
Standard–test pairs of filters for which identification thresholds were significantly higher than discrimination thresholds for at least two observers either in Experiment 1 or 2 (numbers from psychometric curve based hypothesis test are shown in parentheses)

# Observers		Standard (sunlight)	Test (skylight)	# Observers		Standard (skylight)	Test (sunlight)
X	T			X	T		
2(3)	1(1)	Red	Blue	3(3)	2(2)	Blue	Magenta
2(3)	2(2)	Blue	Magenta	1(1)	1(3)	Magenta	Red
2(3)	3(3)	Magenta	Blue	2(2)	2(2)	Blue	Red
2(2)	0(1)	Red	Magenta	1(2)	1(1)	Red	Blue
0(2)	1(0)	Yellow	Green	0(2)	3(1)	Red	Magenta
3(2)	1(1)	Cyan	Blue	1(1)	2(2)	Green	Yellow
				1(1)	1(2)	Blue	Yellow

spectrum, i.e., if one can infer that it will appear white under a spectrally uniform illuminant. In most conditions the object will appear bluish or yellowish or even of variegated colors depending on the illuminant and the interreflections in the scene. In other words, constancy of object colors is "inferred" not "sensed". Without committing ourselves to whether the "inference" is volitional or automatic, in this paper we have introduced a performance based experimental method that measures the veridicality of the inferred colors. The observer is asked to pick identical filters under two different illuminants in the presence of distractors that vary in similarity to the standard. In the conventional task of asymmetric color matching, there is an unavoidable confusion between "sensed" and "inferred" colors (Arend & Reeves, 1986; Marzynski, 1939; Nishida & Shinya, 1998; Zaidi, 2001). In the performance based task the observer has the psychological set of identifying like materials despite obvious differences in appearance. The results of this study show that, in the vast majority of cases, observers' identification performances are limited only by discrimination limens.

4.3. Perceptual transparency and perceptual scission

The majority of studies concerning perceptual scission have been devoted to examining which brightness or color relations across X-junctions are required for the perception of transparency (Beck, 1978; Beck, Prazdny, & Ivry, 1984; D'Zmura et al., 1997; Gerbino et al., 1990; Kersten, 1991; Metelli, 1974). Gerbino et al. (1990), however, have treated transparent layer perception for neutral density filters as a constancy problem. Superimposing transparent layers on two different sets of achromatic backgrounds, they tested whether the opacities of two layers could be matched. Observers adjusted the luminance of overlaid regions of one background set to match the perceived overlay superimposed on the other set. The layer and background components, obtained from the data, corresponded well with the Metelli (1974) episcotister model of non-spectral transparency. Our study extends constancy concerns to the domain of colored filters and objects. D'Zmura, Rinner, and Gegenfurtner (2000) have examined the other side of scission, i.e., constancy of the colors of materials seen behind transparent filters.

In Fig. 1(a), the four circular discs evoke an immediate percept of geometrical and color scission between transparent layers and backgrounds in all our observers. This is not surprising given the presence of abundant cues to transparency, especially X-junctions with the appropriate color relationships (D'Zmura et al., 1997; Kersten, 1991; Metelli, 1974). We tested whether transparency was responsible for enabling filter identification performance, by abolishing all the X-junction cues in Experiment 2. It is worth noting that X-junctions in themselves are not necessary for percepts of transparency, e.g., a filter can be carefully laid on a sparse polka-dotted background such that its edges do not intersect any dots, and thus do not form X-junctions, yet the transparency can be easily visible. In addition, color relationships at the borders of transparent overlays do not have to be physically realistic to evoke perceptual transparency (D'Zmura et al., 1997). However, rotation of the "filtered segments" in Fig. 1(b) also destroys the continuation of the objects passing under the filters, which would be a highly improbable occurrence in natural scenes. Given the similarity of the results for stimuli like Fig. 1(a) and (b), therefore, we are forced to conclude that though the image cues in Fig. 1(a) promote perceptual transparency, they do not improve identification performance beyond that possible solely from chromatic cues. It should be noted that at a large distance, the circular regions in Fig. 1(b) also appear vaguely overlaid. Presumably the border relations are not salient at these distances, and the continuous circular edge of the filtered region provides adequate segmentation.

It is worth noting that our earlier conclusion, that both experiments document the accuracy of inferred color constancy for ensembles of objects, requires color scission between material reflectances and illuminant spectra. We suggest that this color scission is a result of a neural process akin to transformational color matching.

4.4. Discrimination performance

The similarity between the sets of discrimination data from Experiments 1 and 2 shows that geometrical or color relationships at filter borders did not make any difference, and that the thresholds most likely represent the results of discrimination between spatial ensembles of colors. The experiments thus bear a resemblance to the Li and Lennie (1997) work on segregation between chromatic textures. Since the color ensembles on the screen simulated natural materials, illuminants, and filters, these experiments can also be compared to the temporal habituation experiments of Webster and Mollon (1997) that used statistics of natural images. The conjunction of the two properties makes this data set unique in representing color discrimination under semi-naturalistic conditions. Therefore, though this data set does not contain exclusive stimulation of individual color mechanisms (Krauskopf & Gegenfurtner, 1992; Sachtler & Zaidi, 1992; Yeh, Pokorny, & Smith, 1993; Zaidi, Shapiro, & Hood, 1992), we have made an attempt to glean the most salient effects.

We show that under our conditions, discrimination thresholds are systematically different on the sunlight side from that on the skylight side. In Fig. 9, each of the panels corresponds to one of the six standard filters. The

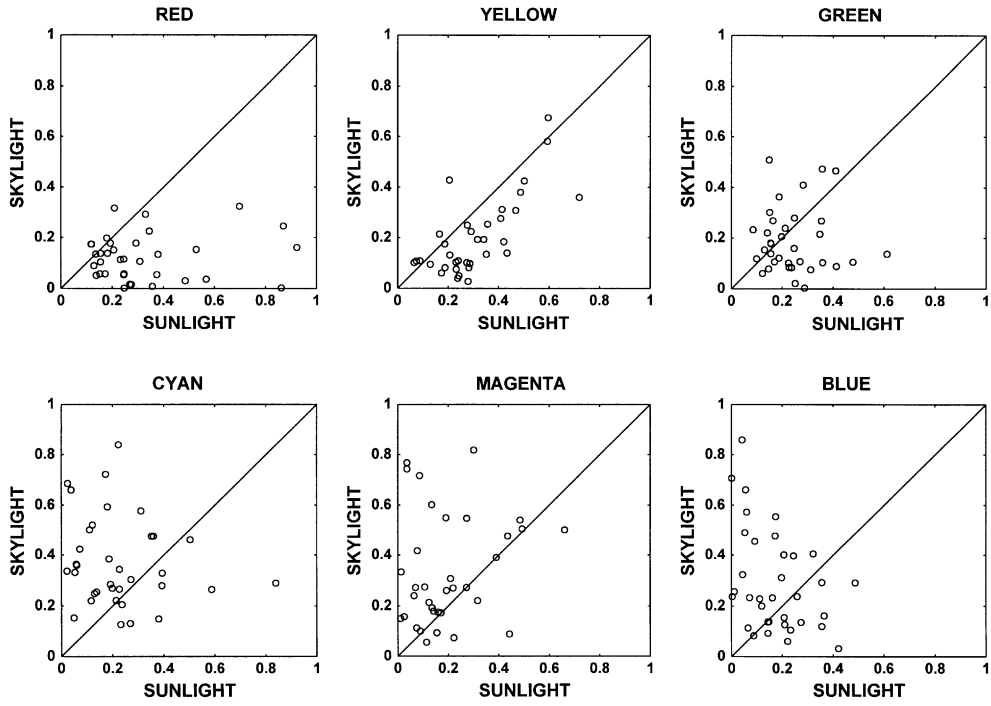

Fig. 9. Discrimination thresholds under skylight versus those under sunlight plotted separately for six standard filters. Each plot includes measurements for all seven observers in the two experiments.

values of discrimination thresholds (in Δ units) under skylight are plotted versus the values of the discrimination thresholds under sunlight for the same standard–test pairs, for all observers in both experiments. Threshold values are higher under sunlight for the red and yellow filters and under skylight for the blue and magenta filters, indicating different adaptation states under the two illuminants. Since Δ units represent spectral differences between overlaid filters, these thresholds could potentially be affected by any or all of the statistical moments of color distributions in the overlaid and exposed regions. Below, we examine the extent to which the means of the color distributions can explain differences between discrimination thresholds, by using published results based on spatially uniform fields.

In published studies of discrimination, three main results predominate. First, in steady state adaptation to spatially uniform fields, it has been long known that thresholds for brightness excursions from the steady level increase monotonically with the steady brightness level, e.g. Craik (1938). Krauskopf and Gegenfurtner (1992) and Zaidi et al. (1992) have shown a similar linear increase for $S/(L+M)$ excursions as a function of steady $S/(L+M)$ level. On the other hand, thresholds for $L/(L+M)$ excursions are constant for all equiluminant $L/(L+M)$ levels (Krauskopf & Gegenfurtner, 1992; Shapiro & Zaidi, 1992; Zaidi et al., 1997). Second, experiments that use flashed pedestals distinct from the adapting stimuli have shown that discrimination thresholds are lowest at the adaptation point and increase on both sides of the adaptation point, forming V-shaped curves (Craik, 1938; Krauskopf & Gegenfurtner, 1992; Shapiro & Zaidi, 1992; Zaidi et al., 1992). The third result is that in the presence of transients there is a selective increase of thresholds along color directions parallel to the transient. This is true whether the transients are created by temporal modulation of the stimulus (Krauskopf, Williams, Mandler, & Brown, 1986; Zaidi & Halevy, 1993; Zaidi & Shapiro, 1993) or by eye movements across spatially variegated fields (Zaidi et al., 1997).

To examine these effects on the discrimination data in Experiments 1 and 2, we have calculated the mean MacLeod–Boynton chromaticity of all objects under the standard filters and test filters at threshold, and plotted them for each illuminant and experimental condition in Fig. 10. The mean material chromaticities under the standard filters are indicated by lower case letters. Lines connect these points to the thresholds for the five test filters each, where the thresholds are the means for the four observers in Experiment 1 and the three observers in Experiment 2. Transformation of the threshold deltas into chromaticity space reveals various aspects of discrimination performance. The overall pattern of the threshold excursions taken by the five test filters paired with a standard filter in the T-junction condition (Experiment 2) were similar to that of the threshold excursions taken by the same five test filters coupled with the same standard filters in the X-junction condition (Experiment 1). This resemblance holds under both

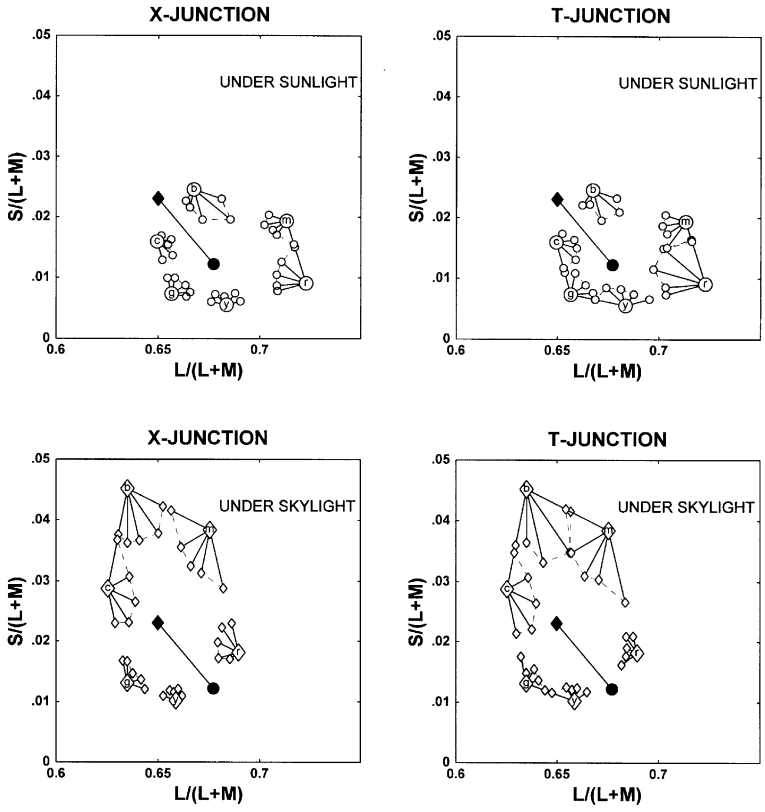

Fig. 10. Horizontal and vertical axes represent the values of $L/(L+M)$ and $S/(L+M)$ in MacLeod and Boynton chromaticity space. Discrimination thresholds in MacLeod and Boynton chromaticity diagram under sunlight and skylight in X- and T-junction image conditions. Means of the materials under the test filters are drawn as open circles connected with mean chromaticity under the standard filter. Filled diamond and filled circle connected by a line segment represent means of the materials' chromaticities under sunlight and skylight with no filter.

sunlight and skylight. Discrimination thresholds under the conditions of this study are considerably higher than thresholds for uniform tests on uniform backgrounds. This result is consistent with previous measurements of large field discrimination thresholds on variegated backgrounds (Zaidi et al., 1997), and the increase of threshold as a function of variance in chromatically variegated fields (Li & Lennie, 1997).

When threshold magnitudes are compared between skylight and sunlight conditions, thresholds from blue, magenta, and cyan standards tended to be larger under skylight than under sunlight, whereas thresholds from red or yellow standards tended to be larger under sunlight than under skylight. This tendency holds for both X-junction conditions (Experiment 1) and T-junction conditions (Experiment 2). Under skylight, the main trend is a monotonic increase in thresholds for excursions in directions close to the $S/(L+M)$ axis, as a function of the $S/(L+M)$ level of the mean chromaticity of the standard overlaid region. This result indicates that S-cone system adaptation was governed by the local overlaid region. If adaptation were governed by the mean background of the illuminated side, $S/(L+M)$ thresholds would increase both above and below the filled diamonds (Krauskopf & Gegenfurtner, 1992; Zaidi et al., 1992). Under sunlight, the main difference is that thresholds to the right of the filled circle (mean of illuminated background) tend to be larger than to the left. This result is inconsistent with published results based on spatially uniform fields (Krauskopf & Gegenfurtner, 1992; Shapiro & Zaidi, 1992), and may reflect the higher variance of $L/(L+M)$ chromaticities under red, magenta, and blue filters (Fig. 4).

In each of the panels of Fig. 10, the filled diamond shows the mean chromaticity of materials under unfiltered skylight, the filled circle shows the mean under sunlight. The line joining these symbols thus indicates the direction of mean color modulation of the background between trials and by eye movements across the vertical illumination boundary as fixation shifts across filters within each trial. The discrimination data in Fig. 10 show a tendency for thresholds from standard filters to be highest for excursions close in angle to the background modulation, e.g., the red–blue and yellow–cyan pairs. These results are consistent with the selective desensitization effects of modulation color direction (Krauskopf et al., 1986; Zaidi & Halevy, 1993; Zaidi et al., 1992; Zaidi et al., 1997). Notice in Fig. 4 (left

column) that the directions of modulations between mean chromaticities across the two illuminants for materials under identical filters are close to parallel to the directions of background modulation.

5. Summary

This paper examines the effects of perceptual scission, image junctions, color adaptation and color correlations on the constancy of inferred transparent overlays. We used simulations of natural illuminants, materials, and filters in a forced-choice procedure to simultaneously measure thresholds for identifying filters and objects across illuminants, and discrimination thresholds within illuminants. The results showed that in the vast majority of the cases, if observers could discriminate within illuminants they could identify across illuminants. Since results were similar for identical color distributions, whether transparency cues like X-junctions were present or not, the primary cues for color identification were assumed to be systematic color shifts across illuminants. We show that these color shifts can be described well by three-parameter affine transformations, and that the parameters can be derived from differences and ratios of mean chromaticities. For the identification strategy we propose a process of post-transformation color matching. This strategy predicts generally accurate identification despite perceptible color shifts, and also provides plausible reasons for those few conditions where identification thresholds were significantly higher than discrimination thresholds.

Acknowledgements

We would like to thank Eun-Sook Kang, Jeannete Meng, and Jeremy Goldmann for patient and careful observations, and Fuzz Griffiths, Andrea Li, Sei-ichi Tsujimura, Jeannette Meng, and Rocco Robilotto for comments on the paper. This work was partially supported by NEI grant EY07556 to Q. Zaidi.

Appendix A. Estimation and hypothesis testing

As stated earlier, the observer's response simultaneously provides percent correct for a pair of independent 2AFC tasks, i.e. choosing (i) the vertical pair which contains dissimilar filters within illuminants, and (ii) the horizontal pair which contains dissimilar filters across illuminants. As such it is a variant of the classical 2×2 detection–discrimination task and can be statistically analyzed by variants of well established procedures (Watson & Robson, 1981). We adopt the following notation:

H	horizontal correct response
$\bar{\text{H}}$	horizontal incorrect response
V	vertical correct response
$\bar{\text{V}}$	vertical incorrect response
δ	index for Δ
n_δ	# of trials at level Δ
$m_{\delta k}$	# of responses in each category at level Δ
$r_{\delta k}$	probability of responses in each category at level Δ
J	# of Δs in each set
$P(\text{I})$	probability of identifying the correct filter
$P(\text{D})$	probability of correct discrimination
P_δ	discrimination probability at Δ
P_V	probability of guessing correct vertical side
P_H	probability of guessing correct horizontal side
f_δ	# of filter-correct responses $= m_{\delta 1}$
s_δ	# of side-correct responses $= m_{\delta 1} + m_{\delta 2}$
$P_{\text{f}\delta}$	probability of picking correct filter at level δ
$P_{\text{s}\delta}$	probability of picking correct side at level δ

There are four possible responses in each trial and k is the index for response categories:

$$\begin{aligned} &k = 1 \Rightarrow \text{V } \& \text{ H}, \qquad k = 3 \Rightarrow \bar{\text{V}} \ \& \ \text{H} \\ &k = 2 \Rightarrow \text{V } \& \ \bar{\text{H}}, \qquad k = 4 \Rightarrow \bar{\text{V}} \ \& \ \bar{\text{H}} \end{aligned} \tag{A.1}$$

The likelihood of getting $m_{\delta k}$ responses is given by the multinomial probability distribution for each Δ:

$$L_\delta = \frac{n!}{\prod_k m_{\delta k}!} \prod_k (r_{\delta k})_{m_{\delta k}} \tag{A.2}$$

The likelihood of the whole data set of Δs for each standard–other comparison is:

$$L = \prod_\delta L_\delta \tag{A.3}$$

The simplest hypothesis about the distribution of $r_{\delta k}$ is H_0: assume nothing about the parameters. Under this hypothesis, the best estimate for each $r_{\delta k}$ is $m_{\delta k}/n_\delta$. The total number of parameters is $3J$ since $\sum_k r_{\delta k} = 1$.

The hypothesis we want to test is H_1: $P(\text{I}|\text{D}) = 1.0$ Since locations of filters, illuminants and materials were randomized across trials, any biases for locations will cancel out, and we can assume that $P_\text{V} = P_\text{H} = 0.5$. The category probabilities can be written as:

$$\begin{aligned} &r_{\delta 2} = r_{\delta 3} = r_{\delta 4} = 0.33(1 - P_\delta) \\ &r_{\delta 1} = 1 - 3r_{\delta 2} \end{aligned} \tag{A.4}$$

Notice that H_1 essentially implies that there should be an equal number of responses in the three error categories.The number of parameters under this hypothesis is J. The maximum likelihood estimate under each hypothesis can be found by maximizing L or $\log L$. For H_0, the estimates are substituted into the likelihood equation. For H_1, a minimizing routine is used. To test whether H_1 fits as well as H_0, we used the statistic:

$$\lambda = -2\ln(L_1/L_0) \tag{A.5}$$

where L_1 and L_0 are the maximum likelihoods under H_1 and H_0. λ is asymptotically distributed as χ^2 with $3J - J = 2J$ degrees of freedom. Since there were six Δ levels, for 12 d.f. at $p > 0.05$, the critical level of χ^2 is 21.0261. If H_1 is not as likely as H_0, then $P(I|D) \neq 1.0$, particularly if $m_{\delta 2} > (m_{\delta 3} + m_{\delta 4})/2$. When the number of trials per Δ level is large, H_1 can be tested by using Pearson's χ^2 goodness of fit criterion to reject or not reject the fit of A4 to the data (Mood & Graybill, 1963).

An alternative method to analyze the data is to fit psychometric curves to the method of constant stimuli data. This has the additional advantage of providing estimates of thresholds for identification and discrimination. In the observer's 4AFC filter identification task, discrimination responses were judged as correct when either filter on the same side (i.e. under the same illuminant) as the test filter was chosen, whereas correct identification required that the test filter be chosen. For each combination of F_s and F_o, the discrimination data consisted of the number of times the correct side was chosen versus Δ, identification data consisted of the number of correct test filter responses versus Δ. Both types of psychometric data were fit by the Quick (1974) function:

$$P = 1 - (1 - \gamma)2^{-(\Delta/\alpha)^\beta} \tag{A.6}$$

where α, β, and γ represent threshold magnitude, steepness, and guessing parameters, respectively. Probability of guessing γ was set at 0.5 for discrimination (two possible sides) and 0.25 for identification (four possible filters). For each of the 60 pairs of discrimination and identification data, the maximum likelihood estimates of α and β were obtained by fitting Eq. (A.6) (Watson, 1979). Maximum likelihood χ^2 tests at $p < 0.05$ indicated that the curves generally fit the data well. The few bad fits were due either to an outlier below threshold, or to chance responding through the whole range indicating that threshold was larger than a Δ of 1.0. Discrimination threshold corresponded to a probability of 0.75 of the side-correct curve, and identification threshold to a probability of 0.625 of the filter-correct curve.

There are two ways that estimated psychometric curves can be used to test whether $P(I|D) = 1.0$. In the method we have employed, we used the derivation below that under hypothesis H_1, there should be a good fit of Eq. (A.6) to both side-correct and filter-correct data with the same α and β, but different guessing parameters.

If $P(I|D) = 1.0$, then:

$$P_{f\delta} = r_{1\delta} = P_\delta + (1 - P_\delta)P_V P_H \tag{A.7}$$

$$P_{s\delta} = r_{1\delta} + r_{2\delta} = P_\delta + (1 - P_\delta)P_V \tag{A.8}$$

Making the usual assumption relating probability of discrimination to analyzer output (Graham, 1989):

$$P_\delta = 1 - 2^{-(\Delta/\alpha)^\beta} \tag{A.9}$$

We obtain the following Quick functions:

$$P_{f\delta} = 1 - (1 - P_V P_H)2^{-(\Delta/\alpha)^\beta} \tag{A.10}$$

$$P_{s\delta} = 1 - (1 - P_V)2^{-(\Delta/\alpha)^\beta} \tag{A.11}$$

We simultaneously fit Eqs. (A.10) and (A.11) to the filter-correct and side-correct data respectively and tested the maximum likelihood χ^2. In those cases where this fit was rejected, but the fits of Eq. (A.6) with separate parameters were satisfactory, we concluded that identification thresholds were significantly higher than discrimination threshold.

An alternative hypothesis testing method would involve separating the data as percent correct for horizontal pairs and percent correct for vertical pairs. The two sets of data could then be fit by independent versions of Eq. (A.6), and also by a simultaneous version. The quality of the simultaneous fit can be compared to the fit of the two separate curves by comparing the likelihoods:

$$\lambda = -2\ln\{L(\text{data}|\text{single curve}) / L(\text{data}|\text{independent curves})\} \tag{A.12}$$

λ is distributed as χ^2 with two degrees of freedom. If λ exceeds the criterion value for $p = 0.05$, the two sets of data do not arise from the same distribution (Sachtler & Zaidi, 1995).

References

Arend, L. E. (1994). Surface colors, illumination and surface geometry: intrinsic image models of human vision. In A. L. Gilchrist (Ed.), *Lightness, brightness and transparency* (pp. 159–214). Hillside, NJ: Lawrence Erlbaum Associates.

Arend, L. E., & Reeves, R. (1986). Simultaneous color constancy. *Journal of the Optical Society of America A*, *3*, 1743–1751.

Beck, J. (1978). Additive and subtractive color mixture in color transparency. *Perception & Psychophysics*, *23*, 265–267.

Beck, J., Prazdny, K., & Ivry, R. (1984). The perception of transparency with achromatic colors. *Perception & Psychophysics*, *35*, 407–422.

Bex, P. J., & Makous, W. L. (2001). Contrast perception in natural images. *Investigative Ophthalmology & Vision Science (Suppl.)*, *42*, S616.

Chen, V. J., & D'Zmura, M. (1998). Test of a convergence model for color transparency perception. *Perception*, *27*, 595–608.

Craik, K. J. W. (1938). The effect of adaptation on differential brightness discrimination. *Journal of Physiology*, *92*, 406–421.

Dannemiller, J. L. (1993). Rank orderings of photoreceptor photon catches from natural objects are nearly illuminant-invariant. *Vision Research*, *33*, 131–140.

D'Zmura, M., Colantoni, P., Knoblauch, K., & Laget, B. (1997). Color transparency. *Perception*, *26*, 471–492.

D'Zmura, M., Rinner, O., & Gegenfurtner, K. R. (2000). The colors seen behind transparent filters. *Perception*, *29*, 911–926.

Faul, F. (1996). Chromatic scission in perceptual transparency. *Perception (Suppl.)*, *25*, 105.

Foster, D. H., & Nascimento, S. M. (1994). Relational colour constancy from invariant cone-excitation ratios. *Proceedings of Royal Society of London (B)*, *257*, 115–121.

Gerbino, W., Stultiens, C. I., Troost, J. M., & de Weert, C. M. (1990). Transparent layer constancy. *Journal of Experimental Psychology: Human Perception and Performance*, *16*, 3–20.

Graham, N. (1989). *Visual pattern analyzers*. New York: Oxford University Press.

Heider, G. M. (1933). New studies in transparency, form and color. *Psychologische Forschung*, *17*, 13–56.

Ives, H. E. (1912). The relation between the color of the illuminant and the color of the illuminated object. *Transactions of the Illuminating Engineering Society*, *7*, 62–72.

Kersten, D. (1991). Transparency and the cooperative computation of scene attributes. In M. S. Landy, & A. J. Movshon (Eds.), *Computational models of visual processing*. Cambridge, MA: MIT Press.

Khang, B., & Zaidi, Q. (submitted). The accuracy of color scission in filter matching: background effects.

KodakCC50 (1962). Kodak Wratten Filters. For scientific and technical use. Rochester 4, NY, Eastman Kodak Company.

Krauskopf, J., & Gegenfurtner, K. (1992). Color discrimination and adaptation. *Vision Research*, *32*, 2165–2175.

Krauskopf, J., Williams, D. R., Mandler, M. B., & Brown, A. M. (1986). Higher order color mechanisms. *Vision Research*, *26*, 23–32.

Li, A., & Lennie, P. (1997). Mechanisms underlying segmentation of colored textures. *Vision Research*, *37*, 83–97.

Lichtenberg, G. C. (1793). Letter to Johann Wolfgang von Goethe on "Farbige Schatten". Translation by Lee, B., Toost, U. & Zaidi, Q. *Color Research and Application*, in press.

MacLeod, D. I. A., & Boynton, R. M. (1979). Chromaticity diagram showing cone excitation by stimuli of equal luminance. *Journal of the Optical Society of America A*, *69*, 1183–1186.

Marzynski, G. Z. P. (1939). Described in Experimental Psychology (87: 42–72) by Woodworth RS. Henry Holt.

Mausfeld, R. (1998). Colour perception: from Grassman codes to a dual code for object and illuminant colours. In W. G. K. Backhaus, R. Kliegl, & J. S. Werner (Eds.), *Color vision: perspective from different disciplines*. Berlin: Walter De Gruyter.

Metelli, F. (1974). The perception of transparency. *Scientific American*, *230*, 90–98.

Mood, A. M., & Graybill, F. A. (1963). *Introduction to the theory of statistics*. New York: McGraw-Hill.

Moulden, B., Kingdom, F., & Gatley, L. F. (1990). The standard deviation of luminance as a metric for contrast in random-dot images. *Perception*, *19*, 79–101.

Nakauchi, S., Silfsten, P., Parkkinen, J., & Usui, S. (1999). A computational theory of color transparency: recovery of spectral properties for overlapping surfaces. *Journal of the Optical Society of America A*, *16*, 2612–2624.

Nieves, J. L., Romero, J., Garcia, J. A., & Hita, E. (2000). Visual system's adjustments to illuminant changes: heuristic-based model revisited. *Vision Research*, *40*, 391–399.

Nishida, S., & Shinya, M. (1998). Use of image-based information in judgments of surface-reflectance properties. *Journal of the Optical Society of America A*, *15*, 2951–2965.

Quick, R. F., Jr. (1974). A vector-magnitude model of contrast detection. *Kybernetik*, *16*, 65–67.

Robilotto, R., Khang, B., & Zaidi, Q. (submitted). Physical and sensory determinants of perceived transparency.

Sachtler, W. L., & Zaidi, Q. (1992). Chromatic and luminance signals in visual memory. *Journal of Optical Society of America A*, *9*, 877–894.

Sachtler, W. L., & Zaidi, Q. (1995). Visual processing of motion boundaries. *Vision Research*, *35*, 807–826.

Shapiro, A. G., & Zaidi, Q. (1992). The effects of prolonged temporal modulation on the differential response of color mechanisms. *Vision Research*, *32*, 2065–2075.

Smith, V. C., & Pokorny, J. (1975). Spectral sensitivity of the foveal cone photopigments between 400 and 700 nm. *Vision Research*, *15*, 161–171.

Taylor, A. H., & Kerr, G. P. (1941). The distribution of energy in the visible spectrum of daylight. *Journal of the Optical Society of America*, *31*, 3.

Ullman, S. (1996). *High-level vision*. Cambridge, MA: MIT Press.

Vrhel, M., Gershon, R., & Iwan, L. S. (1994). Measurement and analysis of object reflectance spectra. *Color Research and Application*, *19*, 4–9.

Watson, A. B. (1979). Probability summation over time. *Vision Research*, *19*, 515–522.

Watson, A. B., & Robson, J. G. (1981). Discrimination at threshold: labelled detectors in human vision. *Vision Research*, *21*, 1115–1122.

Webster, M. A., & Mollon, J. D. (1997). Adaptation and the color statistics of natural images. *Vision Research*, *37*, 3283–3298.

Westland, S., & Ripamonti, C. (2000). Invariant cone-excitation ratios may predict transparency. *Journal of the Optical Society of America A*, *17*, 255–264.

Yeh, T., Pokorny, J., & Smith, V. C. (1993). Chromatic discrimination with variation in chromaticity and luminance: data and theory. *Vision Research*, *33*, 1835–1845.

Zaidi, Q. (1998). Identification of illuminant and object colors: heuristic-based algorithms. *Journal of the Optical Society of America A*, *15*, 1767–1776.

Zaidi, Q. (2001). Color constancy in a rough world. *Color Research and Application*, *26*, S192–S200.

Zaidi, Q., & Halevy, D. (1993). Visual mechanisms that signal the direction of color changes. *Vision Research*, *33*, 1037–1051.

Zaidi, Q., & Shapiro, A. G. (1993). Adaptive orthogonalization of opponent-color signals. *Biological Cybernetics*, *69*, 415–428.

Zaidi, Q., Shapiro, A., & Hood, D. (1992). The effect of adaptation on the differential sensitivity of the S-cone color system. *Vision Research*, *32*, 1297–1318.

Zaidi, Q., Spehar, B., & DeBonet, J. (1997). Color constancy in variegated scenes: role of low-level mechanisms in discounting illumination changes. *Journal of the Optical Society of America A*, *14*, 2608–2621.